

Article

Analyzing Air Pollution and Traffic Data in Urban Areas in Luxembourg

Wassila Aggoune-Mtala  and Mohamed Laib * 

Luxembourg Institute of Science and Technology, 4362 Esch-sur-Alzette, Luxembourg

* Correspondence: mohamed.laib@list.lu

Abstract: Monitoring air quality is gaining popularity in the research community since it can help policymakers make the right decisions for mitigating the negative effects of the ever-increasing pollution in cities. One of the significant sources of air pollution in urban areas is road transport. Assessing and understanding the relationship between urban traffic and local pollutants is crucial to maintaining sustainable urban mobility. This paper presents an exploratory data analysis of air pollution and traffic in some cities in Luxembourg. Furthermore, we studied the link that several pollutants have with other parameters, such as temperature and humidity. The paper also focuses on traffic and offers more insights for sustainable urban mobility.

Keywords: urban air quality; sustainable mobility; urban traffic; time-series clustering

1. Introduction

The assessment of air quality is gaining popularity in the research community since it can enable policymakers to make proper decisions for mitigating the negative effects of the ever-increasing pollution in cities. Among the different sources of pollution in urban areas, transportation represents a share of almost twenty percent of the overall greenhouse gas emissions (GHGs). Road transportation accounts for the most significant proportion of the total transport emissions (72% of all domestic and international GHG emissions in 2019, according to [1]). As a result, most existing and planned measures in the member states concentrate on road transportation. In parallel, the European Environment Agency's report series on the air quality in Europe provides annual assessments of air pollutant emissions and concentrations in ambient air across Europe and the associated health and environmental impacts [2]. The annual assessments are based on official data from European countries and those following the ambient air quality directives of the European Union (EU), which define the standards for assessing key air pollutants in a given region [3]. These air quality guidelines were derived from those of the World Health Organization (WHO), which published new guidelines in 2021 [4] following a systematic review of the most recent scientific evidence demonstrating how air pollution harms human health. Some European countries have established an air quality index (AQI), a nationally uniform index for reporting and daily forecasting, to provide citizens with information about air quality. It is based on the five most common regulated ambient air pollutants:

1. Particulate matter (PM₁₀) describes inhalable particles with diameters of 10 micrometres and smaller;
2. Nitrogen dioxide (NO₂) is a highly reactive gas that primarily gets into the air from the burning of fuel;
3. Ozone (O₃) is a highly reactive gas composed of three oxygen atoms. Ground-level ozone, which we can breathe, is formed primarily from photochemical reactions between two major classes of air pollutants: volatile organic compounds (VOC) and nitrogen oxides (NO_x);



Citation: Aggoune-Mtala, W.; Laib, M. Analyzing Air Pollution and Traffic Data in Urban Areas in Luxembourg. *Smart Cities* **2023**, *6*, 929–943. <https://doi.org/10.3390/smartcities6020045>

Academic Editor: Pierluigi Siano

Received: 17 January 2023

Revised: 7 March 2023

Accepted: 8 March 2023

Published: 12 March 2023



Copyright: © 2023 by the authors. Licensee MDPI, Basel, Switzerland. This article is an open access article distributed under the terms and conditions of the Creative Commons Attribution (CC BY) license (<https://creativecommons.org/licenses/by/4.0/>).

4. Carbon monoxide (CO), which is a colourless, odourless gas that can be harmful when inhaled in large amounts. CO is released when something is burned. The greatest sources of CO in outdoor air are cars, trucks and other vehicles or machinery that burn fossil fuels;
5. Sulfur dioxide (SO₂), which results from the burning of either sulfur or materials containing sulfur. SO₂ emissions lead to the formation of other sulfur oxides, which can react with other compounds in the atmosphere to form small particles. Short-term exposures to SO₂ can lead to respiratory problems.

The AQI, see Figure 1, informs the public about how clean or polluted the air is and how to avoid potential health consequences. The work in this paper assesses traffic-related air quality using pollutant values.

Pollution	Index	Main Pollutants			Other Pollutants	
		NO ₂	O ₃	PM ₁₀	CO	SO ₂
Very high	>100	>400	>240	>180	>2500	>500
high	100	400	240	180	2500	500
	76	201	181	91	1251	301
Moderate	75	200	180	90	1250	300
	51	101	121	51	938	101
Weak	50	100	120	50	937	100
	26	51	61	26	626	51
Very weak	25	50	60	25	625	50
	0	0	0	0	0	0

Figure 1. European Air Quality Index: the pollutants are expressed in terms of their maximum hourly value in micrograms per cubic meter of air.

Several research initiatives have been proposed to limit the negative effects of pollution on the urban environment. This concerns, for instance, advanced optimization algorithms [5,6] for mobility [7,8] or freight transportation using cleaner vehicles [9–11]. In the framework of smart cities, other works are concerned with the optimization of waste collection [12] or water distribution [13] using Internet of Things (IOT)-based devices. In [14], acoustic sensors were used for monitoring noise annoyance. Most of the publications in the literature regarding smart cities are concerned with the use of advanced technologies, such as IOT devices, or artificial intelligence to measure and monitor pollution. The impact of such initiatives has to be assessed in order to increase the socio-economic benefits of setting up a smart city [15,16]. Still, research that assesses a part of the implemented solutions is relevant, such as [17] for sensors and [18] for machine learning techniques. Indeed, the use of data-driven approaches are of critical importance to reduce the negative effects of several pollutants by defining some essential steps [19]. Furthermore, understanding the source of some pollutants is crucial for informing emission-reduction policies and helping to ensure that the most appropriate air pollution sources are targeted [20]. Several studies have been performed with the aim of understanding the temporal behavior of pollution data and their characteristics [21–23], considering the non-stationarity and non-linearity of pollution data [24]. Many time-series methods have been applied, such as rescaled range analysis for investigating persistence in large urban areas [25,26]. Detrended fluctuation analysis has been undertaken for identifying long-term memory effects and the study of asymmetries in long-term correlations [27]. Complexity measures have also been achieved in order to understand the dynamics of some pollutants [28–30].

In a recent paper, Amato et al. studied the time series of some pollutants, including NO₂ and O₃, that were collected in different areas in Switzerland, using Fisher–Shannon measures and time-series clustering [31]. Their findings pointed out different time-series behaviors depending on where the data were collected (urban environments with traffic, suburban areas, high-mountain regions, etc.).

In this paper, we investigated air pollution data with regard to temperature and humidity. In fact, we considered air pollution time series as data points, to which we applied clustering techniques. The obtained clusters delivered more insights about each pollutant and the local climate. In addition, we explored the weekly behavior of each pollutant and then tried to explain the relationship with the amount of traffic near the sensors. The remainder of the paper is organized as follows. Section 2 describes the collected data and presents a comprehensive exploratory data analysis of air pollution and traffic in some cities in Luxembourg. In Section 3, we perform time-series clustering and describe the links that several pollutants have with other parameters, such as temperature, humidity and the amount of traffic. In Section 4, we give conclusions, as well as perspectives for future works.

2. Data Description

Several sensors have been settled for air quality assessment and traffic counters in several urban areas in Luxembourg. More precisely, these sensors of different natures can measure air pollutant concentrations, temperature, humidity and noise intensity, as well as count and identify vehicles. Their installation depends on the will of the company installing the sensor or the public or private institution near to where a sensor is installed. For instance, seven traffic sensors were installed at the beginning of July 2022, while five air quality sensors were installed in June.

2.1. Air Quality Data

The pollution data used in this paper were collected from five electrochemical air quality sensors named Sensor 1 to Sensor 5. They use LoRaWAN communications, enabling each IoT device to connect over a secure network to one central gateway. This form of communication removes the need for data sim cards, therefore reducing their costs. The sensors collect data every minute from Monday to Friday and from 7 to 9 a.m and from 5 to 7 p.m on those days. The location of the air quality sensors is given in Figure 2 (by the blue circles). Another view is possible at the sensor provider's website via a live map. Two sensors were located in the commune of Nieder Korn (Sensor 1 and Sensor 3 are denoted as S1 and S3 in the figure, respectively), two others were in Differdange and the last one, the Sensor 5 (denoted as S5 in the figure), was located in Oberkorn. The data records for several pollutants, nitrogen dioxide, sulfur dioxide and ozone gases in micrograms per cubic meter (mg/m^3) and carbon monoxides in parts of gas per billion parts of air (ppb), are available. A drop-down menu at the sensor provider's site enables the request of data in a certain period. One can, for instance, choose to observe the record of data for one day, one week or a more extended period. These data can be downloaded in SVG, png or CSV format. For instance, Figure 3 shows the records of the data on climate condition from Sensor 1 in week 27 in png format (from 4 July at 22.00 to 11 July at 12.00).

2.2. Traffic Data

The traffic data were generated by two types of sensors: some acoustic ones and others based on image processing.

2.2.1. Acoustic Sensors

Five acoustic sensors counted the traffic in Differdange and the surrounding area. They relied on Doppler radars. These specialized radars use the Doppler effect to generate velocity data about distant objects. They accomplish this by bouncing a microwave signal off a target and analyzing how the object's motion affects the frequency of the returned signal. The location of these sensors is given in Figure 2 (by the red circles). Visualizing the sensors' data at the sensor provider's site was possible. This way, it enabled to monitor the real-time traffic in key locations of the commune. We could obtain data on the total number of vehicles during each hour that came from either the right or the left direction. The data were available from 13 June onwards. For instance, Figure 4 gives the total number of

vehicles that were recorded by the IKN04 sensor during one month from 22 August to 22 September. Let us note that this sensor was located in the same street as Sensor 1, which measured the air quality. It also gave the vehicles' split depending on their direction from right to left or from left to right.

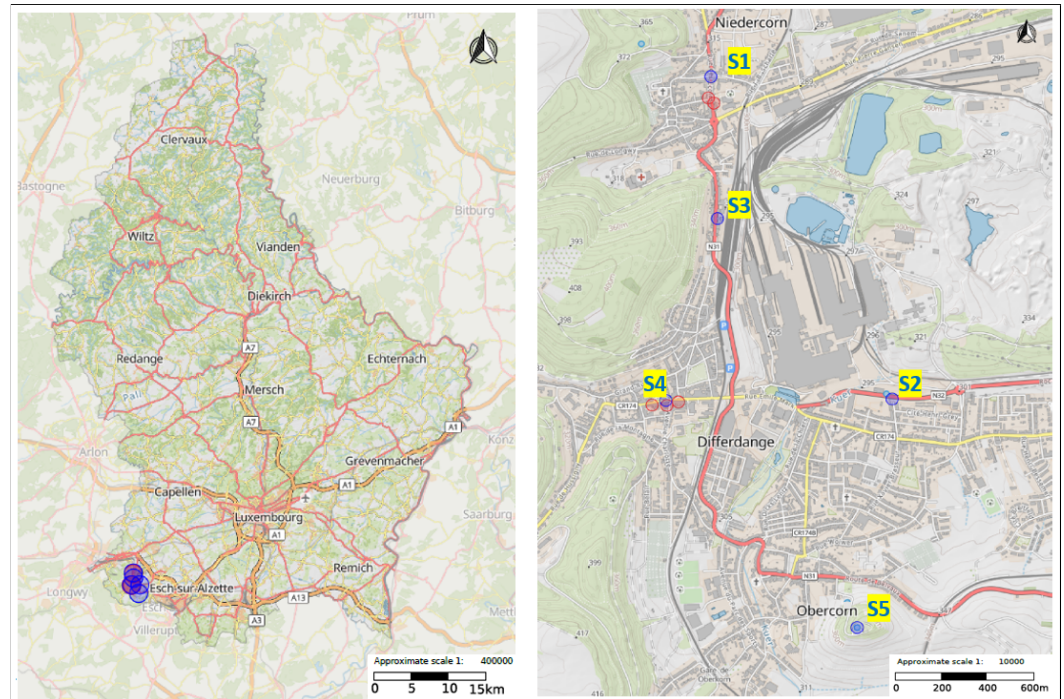


Figure 2. Location of the different sensors used in this paper: the right panel shows more precisely the location of the blue sensors (S1 to S5) for air quality measurements and the red ones for collecting traffic data. The map was generated using Luxembourg's national official geoportal (<https://www.geoportail.lu>) (accessed on 11 January 2023).

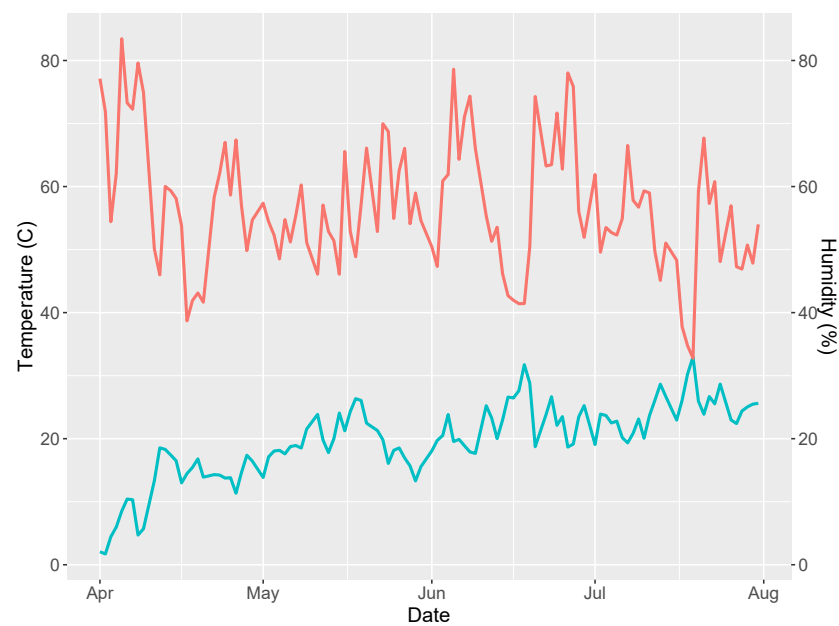


Figure 3. Visualization of the climate conditions recorded by Sensor 1. The blue line indicates temperature, while the red line shows humidity.

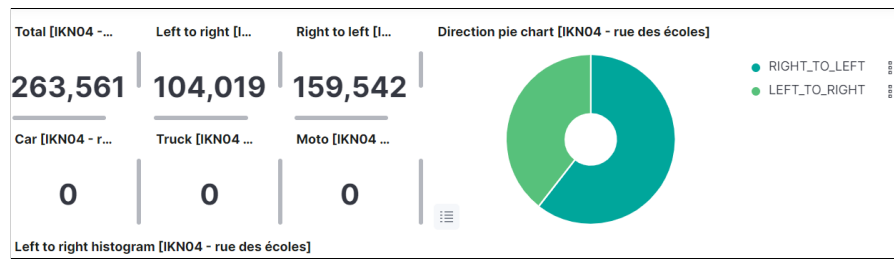


Figure 4. Total number of vehicles from 22 August until 22 September recorded by the sensor IKN04.

We could also obtain the number of vehicles that traversed the road every twelve hours for one month or more. The vehicles that went from the left to the right, and were captured by sensor IKN04 from 22 August until 22 September, are represented in Figure 5.

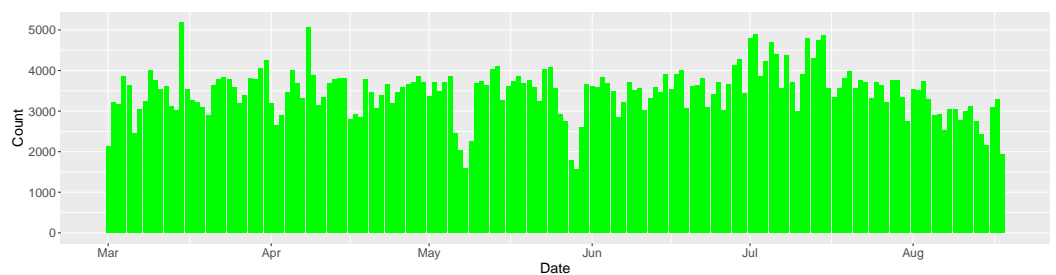


Figure 5. Count of vehicles recorded by the IKN04 sensor from 22 August until 22 September.

2.2.2. Object Detection Sensors

The second type of traffic sensor was the “Telraam” device. Each one was attached to the inside of a window and needed to face the street. The camera took a pixelated image in low resolution, then these images were transmitted to a Raspberry Pi minicomputer, which analyzed them: it could detect objects and their size, speed and location. Finally, an object’s properties were forwarded to a central database where they were converted into one of the four vehicle types. In order to be able to forward the traffic count data to the central database immediately, the device was continuously connected to the Internet via Wi-Fi. The sensor provider gives the location of the Telraam sensors at the following url: <https://telraam.net> (accessed on 11 November 2022), see also Figure 6.

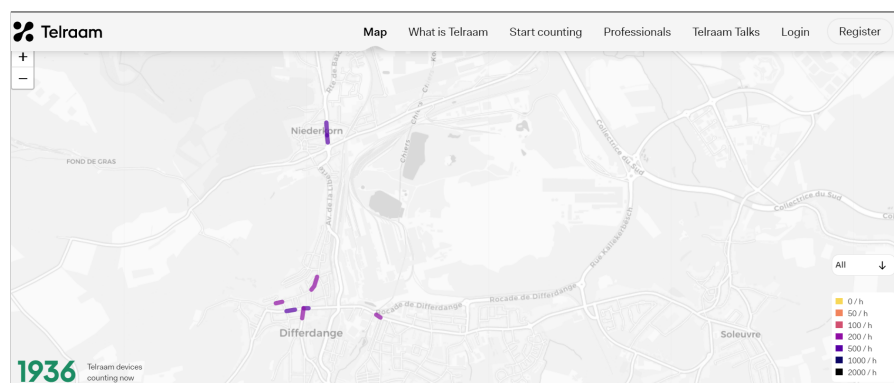


Figure 6. Locations of the eight Telraam sensors.

The Telraam sensors can detect a pedestrian or a vehicle that crosses the road from the left to the right or in the opposite direction, whether its a two wheeler, a car or a heavy vehicle. Figure 7 gives, for instance, the split of the different types of road users from the period starting on 22 August and ending 22 September that was recorded by a sensor located near Sensor 4.

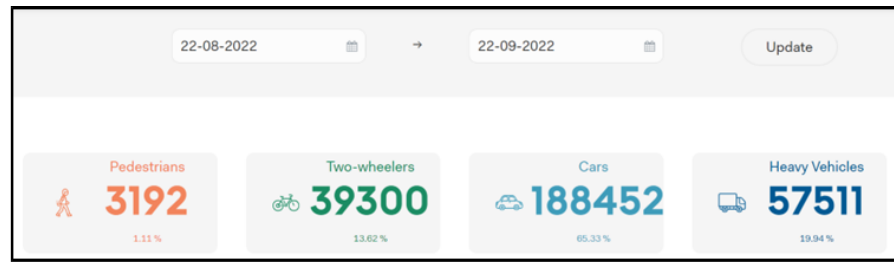


Figure 7. Total number of vehicles per type recorded by the sensor near Sensor 4 for a one month period.

Figure 8 shows the daily traffic count for cars, pedestrians, two-wheelers and heavy vehicles that was recorded by the sensor near Sensor 4 from 22 August until 22 September 2022.

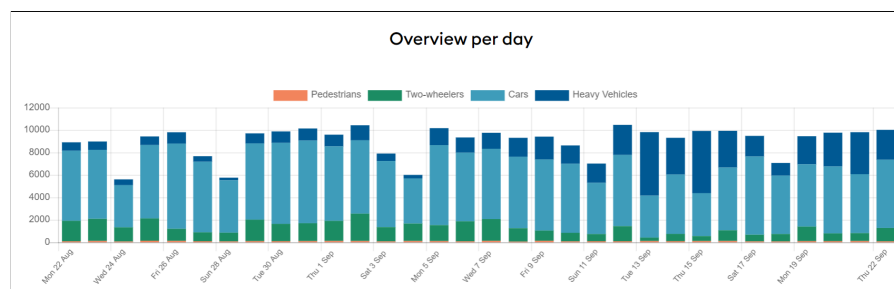


Figure 8. Overview of the traffic per day recorded by the sensor close to Sensor 4 from 22 August until 22 September.

It is also possible to observe, for each hour, the split per category of vehicles and directions recorded by any Telraam sensor, as is the case in Figure 9.

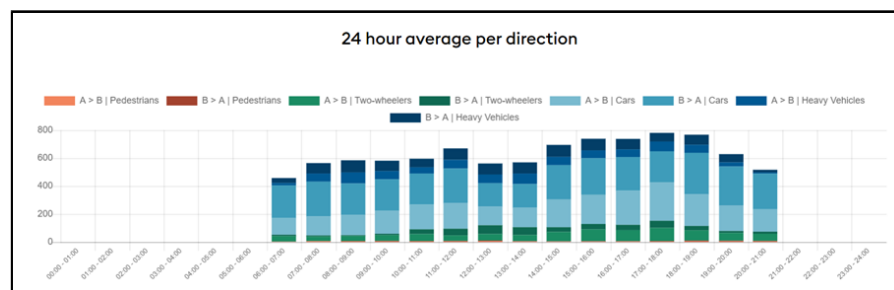


Figure 9. Average per hour of the split per category of vehicles and per direction recorded by the sensor close to Sensor 4 from 22 August until 22 September. A > B represents the direction from the left to the right, and B > A represents the opposite direction.

Lastly, the V85 was also recorded, see Figure 10. This corresponds to the vehicle traffic law where the legal speed limit of a motorway is decreased by 15% in case of hazardous weather conditions [32]. This is common practice in many countries within the European Union [33].

One can observe that the speed limitation was respected during all of the observed period. As some traffic sensors were installed after the air quality ones, data were collected only for the period during which all the sensors were operational. Only the data of the sensors located at the same location as the air quality sensors were considered to assess the impact of the traffic on the air quality.

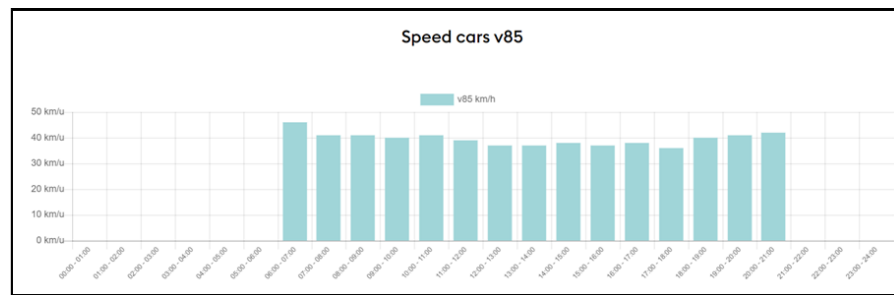


Figure 10. Average speed limit (V85) per hour in the period from 22 August until 22 September recorded by the sensor close to Sensor 4 in Differdange.

2.3. Differentiation of the Collected Data

Daily sensor data averaged over four months were examined in this study (from 1 April to 31 July 2022). Table 1 gives an overview of the data available at the time of the study, an instance being the data recorded on a whole week by one sensor.

Table 1. Data statistics of the studied area.

Air quality	Sources	5
	Instances	320
Weather	Sources	5
	Instances	160
Traffic count	Sources	13
	Instances	208

Figure 11 shows an example of raw data from one of the air quality sensors in Nieder Korn. As is mentioned in the figure, data from the four months (since the beginning of the recording) for four pollutants, namely NO₂, SO₂, O₃ in mg/m³ and CO in ppb, were investigated.

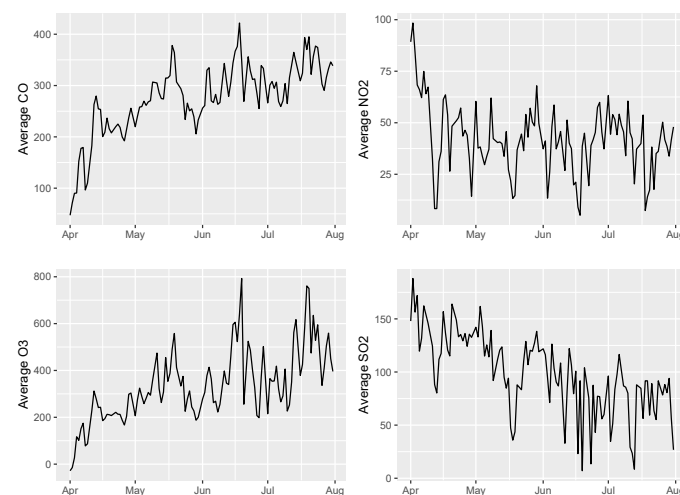


Figure 11. Examples of time series of NO₂, SO₂, O₃ in mg/m³ and CO in ppb that were recorded by one of the sensors in Nieder Korn.

One can easily see the increasing trend of some pollutants, such as the CO and the O₃. We differentiated the time series to remove this trend and other potential seasonalities. Figure 12 shows the results of the differentiation of the time series of Figure 11.

To illustrate the performed differentiation, Figure 13 shows the cross-correlation of SO₂ between sensors (before and after removing the trend and seasonalities). By removing

the trend and the seasonalities, we focused on the local behaviors of the data, which could help to understand, at an urban level, the temporal evolution of these pollutants.

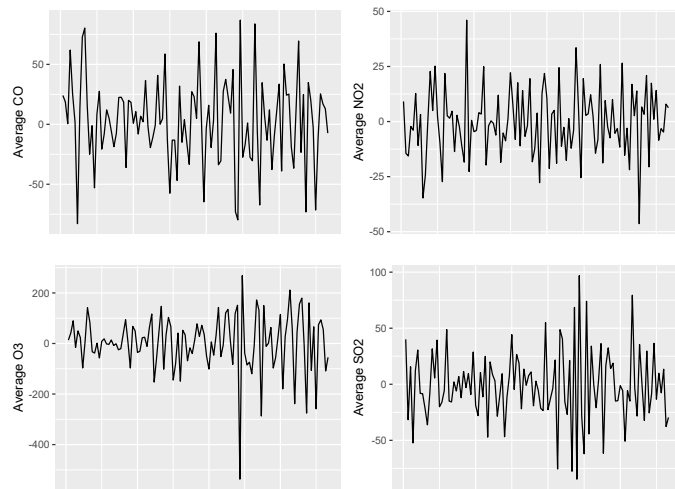


Figure 12. Example of the pollutants' time series (NO_2 , SO_2 , O_3 in mg/m^3 and CO in ppb) from the same sensor in Niederkorn, after differentiation to remove the trend and seasonalities.

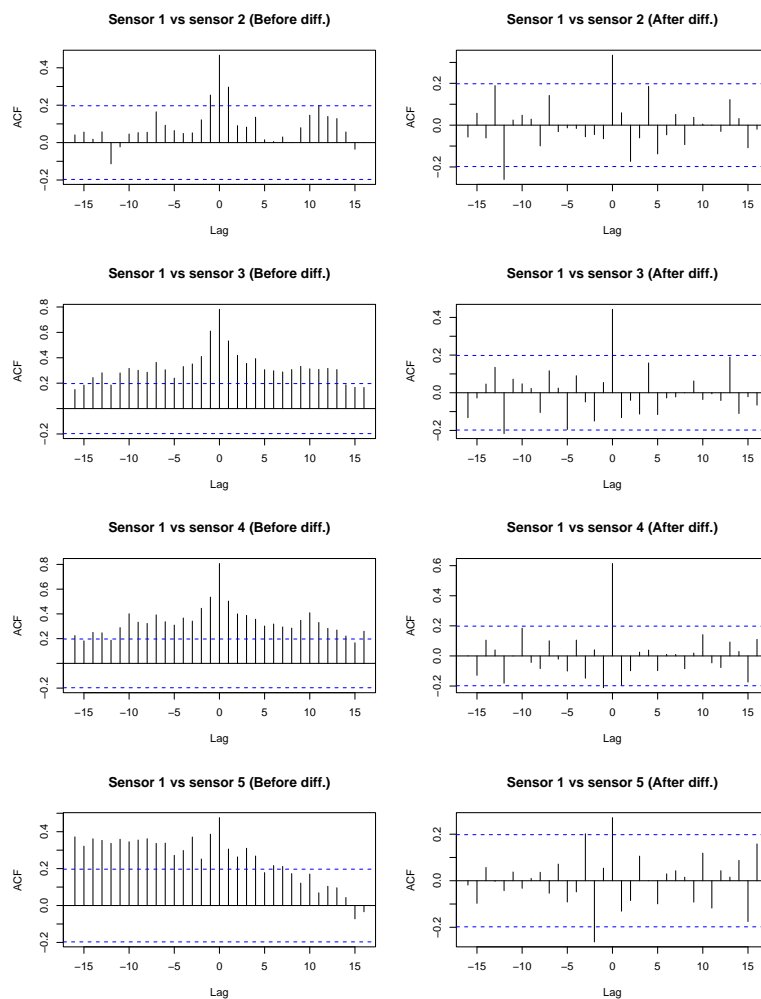


Figure 13. The SO_2 pollutant used as an example to show the high correlation at several lags, between the first sensor and the other four sensors (left-hand-side plots). This correlation was then reduced by differentiating the time series (right-hand-side plots).

3. Time-Series Clustering

3.1. Description of the Method

In many cases, the collected data were not labelled or were lacking information regarding their partition. Unsupervised learning techniques are usually used to overcome this issue [34]. In time-series data, assigning labels is an active research area [35]. The key component in time-series clustering is the choice of a suitable dissimilarity measure. Montero and Vilar suggested an R library (TSclust) that dealt with this issue, in which they offered many dissimilarity techniques [35]. Once the dissimilarity measure is selected, the clustering can be performed using the centroid-based technique (k-means algorithm) [36] or the medoid-based method (partitioning around medoids (PAMs) algorithm) [37]. In this paper, we used a k-means algorithm to perform the clustering. It defined the partition by reducing the sum of the squared errors between the empirical means of each partition and data points belonging to it [38]. Initially, the k-means algorithm randomly defined a partition and then labeled each data point with the closest cluster centre. This procedure was repeated until convergence. The selection of the number of clusters, k , is a crucial step in k-means clustering. There are several methods to select k , including the elbow method [34], in which the sum of the squared distances between each data point and its cluster centroid (also known as the within-cluster sum of squares or WCSS) for different values of k is plotted. The plot will typically form an elbow shape, and the number of clusters can be chosen at the elbow point where the decrease in the WCSS begins to level off. Another method for selecting k is the silhouette method, which measures how well each data point fits into its assigned cluster compared to other clusters. The number of clusters can be chosen to maximize the average silhouette score. Hierarchical clustering can also be used to obtain a dendrogram to choose the number of clusters based on the height of the branches in the dendrogram [34]. The clustering strategy follows the same strategy as in [31]. However, as an example, we show the result obtained by the most straightforward dissimilarity measure, which is a correlation-based dissimilarity [39]. In the next section, time-series clustering is applied to the full time series to evaluate the temporal behavior of each pollutant with respect to the temperature and the humidity.

3.2. Temporal Behavior of Each Pollutant with respect to the Temperature and the Humidity

In Figure 14, one can observe that two clusters of SO₂ data appear for the temperature. The first cluster, in green, is composed of the data captured by four sensors (Sensor 1 to Sensor 4), while the other is composed of data from Sensor 5. There are also two clusters for the humidity, the first one with data from four sensors, Sensor 1 to Sensor 4, and the second, in red, with data from Sensor 5. One can observe a slight difference in humidity and temperature between the two clusters. One can see that Sensor 5 forms, by itself, a cluster and shows slightly different temperature and humidity values compared to the other sensors. Furthermore, the cluster containing Sensor 5 could possibly be influenced by the presence of manufacturers or different activities.

The same trend was observed with the other pollutants. Figures 15–17 represent the clustering of the data for the CO, NO₂ and O₃ pollutants, respectively. There were always two clusters, but they depended on the observed pollutants. For CO and temperature, the first cluster consisted of data from three sensors (Sensor 1 to Sensor 3), while the second contained data from two sensors, Sensor 4 and Sensor 5. Humidity clusters were formed similarly to the temperature clusters.

For the NO₂ data in correlation with the temperatures registered, the first cluster contained data from Sensor 1, Sensor 2 and Sensor 3, which were similar to those of the CO pollutant. The second cluster gathered data from Sensor 4 and Sensor 5. For the humidity, the two clusters had data from the same sensors as for the temperatures. Regarding the O₃ data, two clusters appeared, the first including data from Sensor 1, Sensor 4 and Sensor 5, which had the same temperature behavior. The second cluster was made up of data from Sensor 2 and Sensor 3. The data correlated to humidity resulted in two clusters with data

from the same sensors (Sensor 1, Sensor 4 and Sensor 5) for the green cluster and Sensor 2 and Sensor 3 for the red cluster.

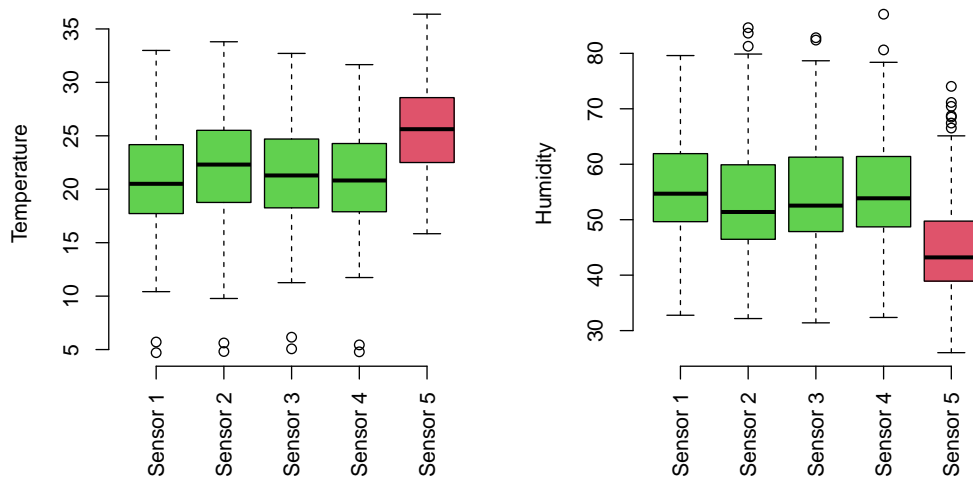


Figure 14. Clustering of SO₂ data for the full period of the study and their visualization with respect to temperature and humidity.

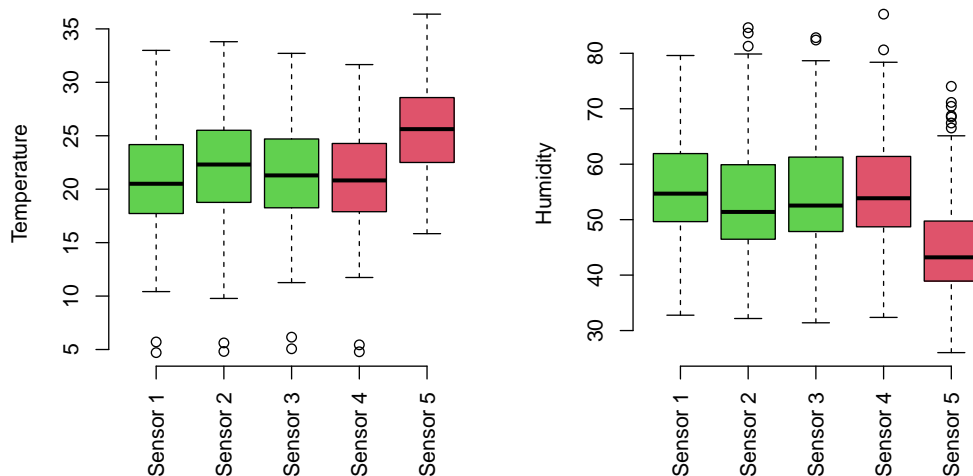


Figure 15. Clustering of CO data for the full period of the study and their visualization with respect to temperature and humidity.

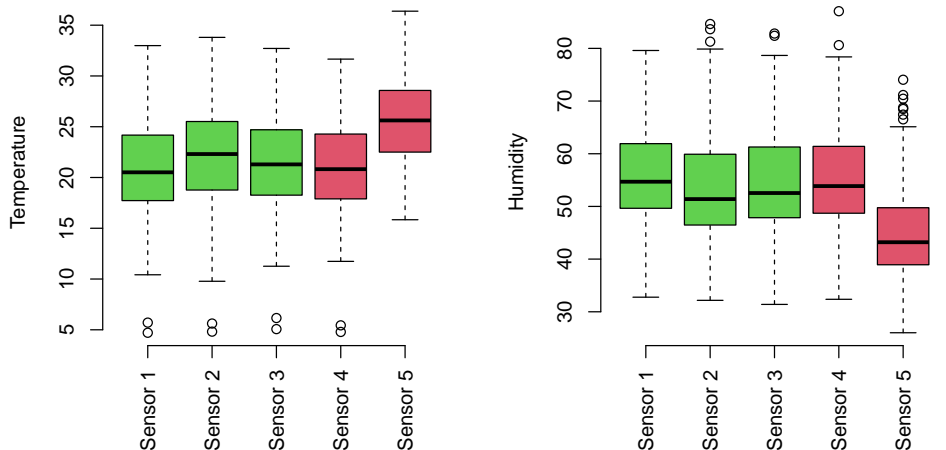


Figure 16. Clustering of NO₂ data for the full period of the study and their visualization with respect to temperature and humidity.

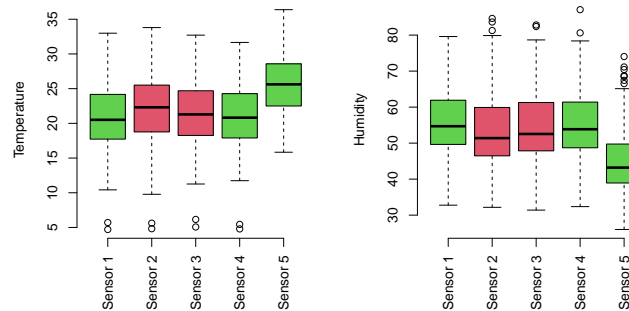


Figure 17. Clustering of O₃ data for the full period of the study and their visualization with respect to temperature and humidity.

3.3. Temporal Behavior of Each Pollutant with Respect to the Traffic

This section reports the results obtained by applying the clustering technique to the whole time series to assess the role of traffic on each pollutant. The same clustering strategy was applied after differentiating the time series from one of the sensors. We grouped the time series by weeks and tried to find clusters. From the recorded 16 weeks, we obtained 4 clusters, each representing the data of several weeks. Figure 18 illustrates how these four clusters were distributed in terms of SO₂ and traffic recorded during these weeks. For each cluster, we computed the median value for visualization purposes. One can see that Cluster 1 and Cluster 2 correspond to a higher amount of traffic and higher values of SO₂. However, Cluster 3 and Cluster 4 show less traffic and a lower value of SO₂ than in the previous clusters.

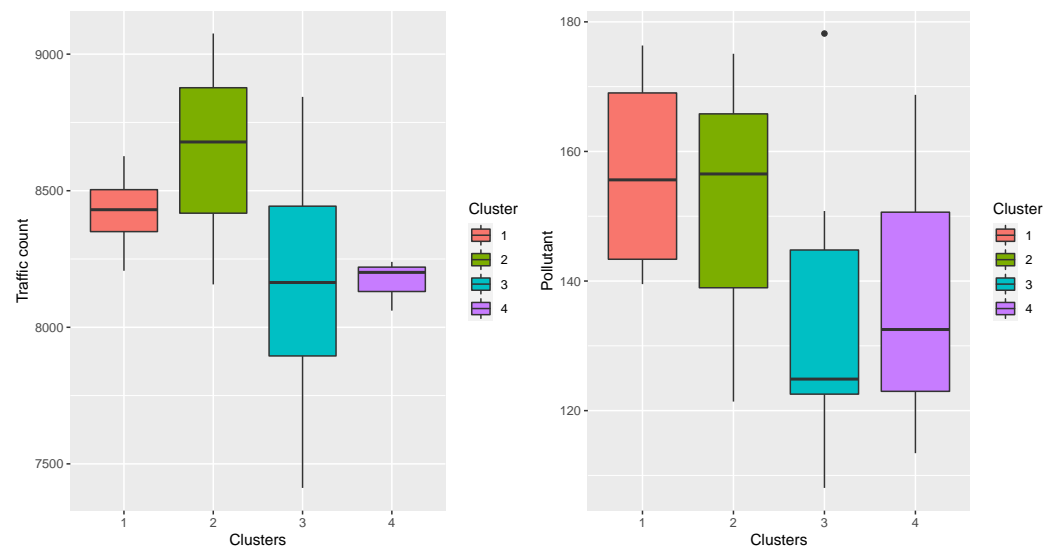


Figure 18. Clustering results applied to several weeks of data and visualization of SO₂ and traffic data.

Figure 19 shows nine clusters of CO and traffic data. One can observe that, for several clusters, the high level of traffic can be linked with the high amount of CO recorded. However, this was not the case for Clusters 1, Cluster 2, Cluster 8 and Cluster 9, which represent almost half of the data.

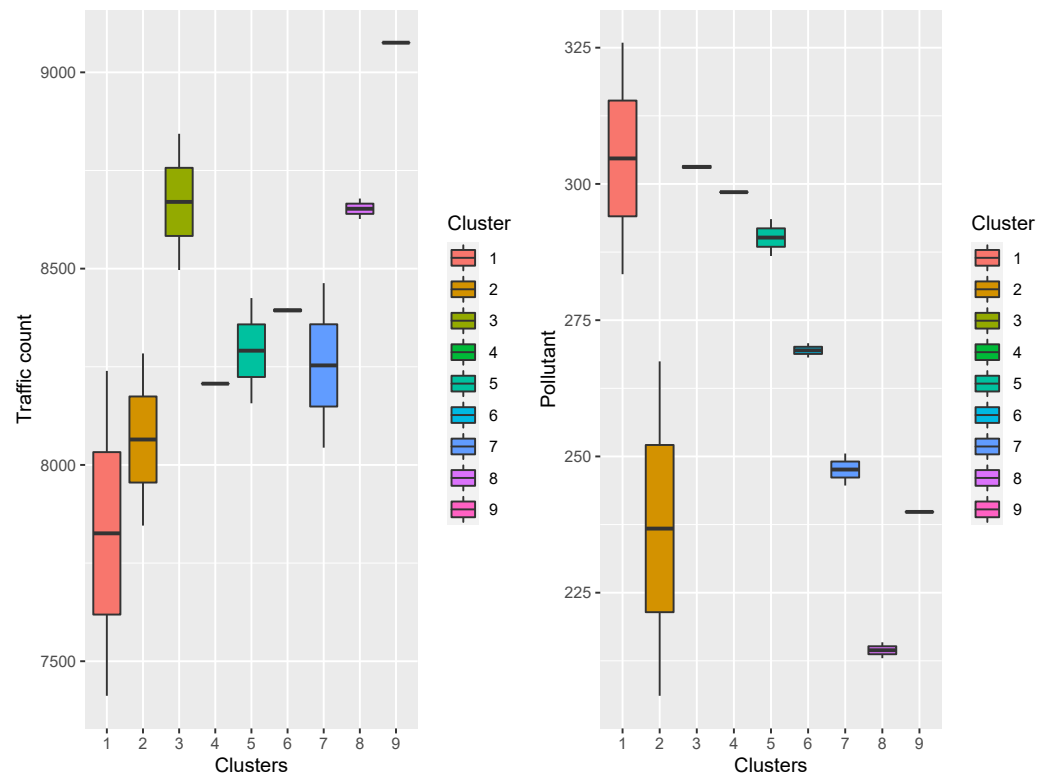


Figure 19. Clustering results applied to several weeks of data and visualization of CO and traffic data.

Figure 20 shows four clusters for the NO₂ pollutant. One can see that for Cluster 1, Cluster 2 and Cluster 4, the distribution of the level of traffic and amount of emitted NO₂ is completely different, which is not the case for the Cluster 3. Globally, the amount of NO₂ tends to be as high as the traffic level.

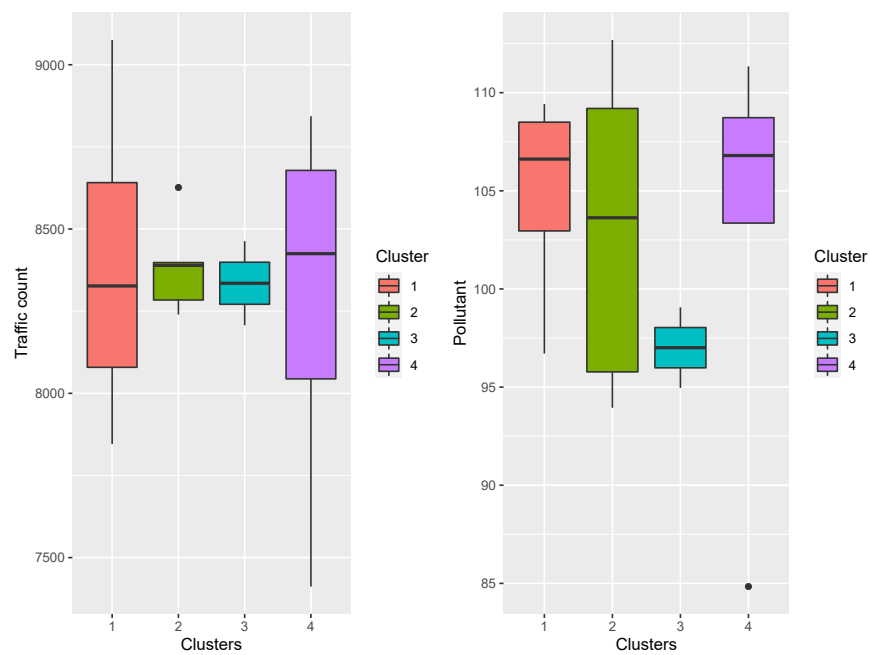


Figure 20. Clustering results applied to several weeks of data and visualization of NO₂ and traffic data.

The results for the O₃ pollutant are illustrated by Figure 21, which shows seven clusters. The data distribution was different for the pollutant and traffic in almost all the clusters. The amount of traffic did not reflect the pollution level in the two first clusters.

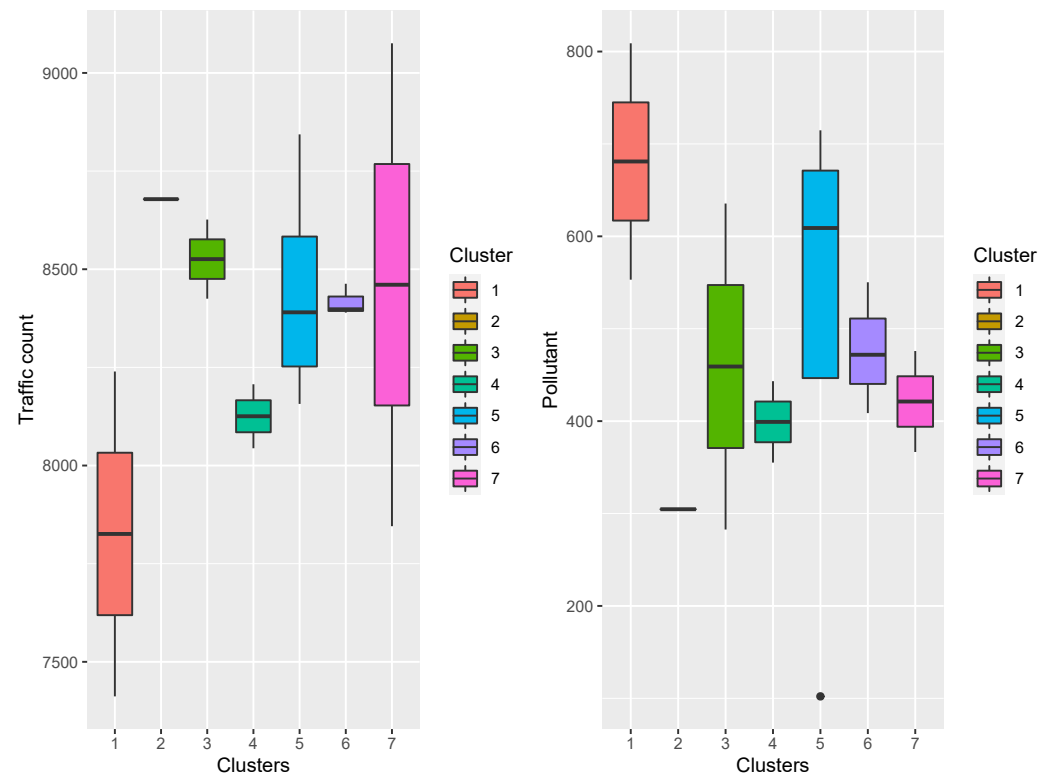


Figure 21. Clustering results applied to several weeks of data and visualization of O₃ and traffic data.

Therefore, despite the results showing a difference in the obtained clusters (concerning temperature, humidity and traffic), it was not easy to point out a causality between these inputs and the different pollutants. For instance, for the traffic, the differences that Cluster 1, Cluster 2 and Cluster 3 have in comparison with the other clusters is clear. However, other related activities could have driven both variables, the traffic and O₃.

4. Conclusions and Perspectives for Future Works

In this work, daily air pollution time series of NO₂, CO, SO₂ and O₃ from five locations in Luxembourg were analyzed and compared with humidity, temperature and traffic data. An exploratory time-series analysis was performed, which showed an increasing trend in some pollutants. Trends and seasonalities were removed by differentiating each time series. Such detrending helped us to focus on the local behaviors of the recorded time series. Clustering was performed to find grouped labels. The clustering explored the potential link between the pollutants and other variables, such as temperature, humidity and the amount of traffic near the recording sensors. The clustering was performed using the k-means algorithm with Pearson correlation as a dissimilarity measure.

As mentioned previously, although the results showed separate clusters concerning urban traffic, the decision to mitigate traffic should consider more parameters. The existing link of pollutants with traffic may be driven by other features to which we presently do not have access, such as the impact of industrial areas near the sensors.

Although the results were interesting, the paper could have been more extensive in terms of purpose because of the amount of data. This work used data recorded only during peak hours during the day, which was also essential to assess the impact of traffic. The data were recorded by a limited number of sensors that covered a small region. However, the proposed methodology could easily be adapted to a more significant number of sensors

covering a wider geographical area. Moreover, this work represents a starting point for an exploratory analysis of the data collected through these sensors. We plan to forecast these time series and the air quality index when more data are collected, mainly when all seasons have been recorded. We will then design an optimization framework to reduce the number of vehicles, for instance, according to environmental parameters and the prediction of pollutant time series. Further works could also involve collecting more features, such as land use, land cover, vegetation, wind speed and information about the city (e.g. building heights) over an extended period.

Author Contributions: Conceptualization, W.A.-M.; Methodology, W.A.-M. and M.L.; Formal analysis, M.L.; Data curation, M.L.; Writing—original draft, W.A.-M.; Writing—review & editing, W.A.-M. and M.L.; Visualization, M.L.; Project administration, W.A.-M. All authors have read and agreed to the published version of the manuscript.

Funding: This project work received funding from the European Union’s Horizon 2020 Research and Innovation programme under grant agreement No. 872548. This support is fully acknowledged.

Acknowledgments: The authors thank both teams from LuxMobility and LIST who were involved in discussions about the DIH4CPS project. The authors are grateful to the anonymous reviewers.

Conflicts of Interest: The authors declare no conflict of interest.

References

1. European Environment Agency. *Greenhouse Gas Emissions from Transport in Europe*; European Environment Agency: Copenhagen, Denmark, 2021.
2. European Environment Agency. *Air Quality in Europe 2021*; European Environment Agency: Copenhagen, Denmark, 2021; Volume 15/2021. [CrossRef]
3. European Environment Agency. Directive 2008/50/CE du Parlement Européen et du Conseil du 21 mai 2008 Concernant la Qualité de l’air Ambiant et un Air pur Pour l’Europe. 2008. Available online: <http://data.europa.eu/eli/dir/2008/50/oj> (accessed on 12 January 2023).
4. World Health Organization. *WHO Global Air Quality Guidelines: Particulate Matter (PM2.5 and PM10), Ozone, Nitrogen Dioxide, Sulfur Dioxide and Carbon Monoxide*; World Health Organization: Geneva, Switzerland, 2021; p. 273.
5. Aggoune-Mtalaa, W.; Aggoune, R. An optimization algorithm to schedule care for the elderly at home. *Int. J. Inf. Sci. Intell. Syst.* **2014**, *3*, 41–50.
6. Djenouri, Y.; Habbas, Z.; Aggoune-Mtalaa, W. Bees swarm optimization metaheuristic guided by decomposition for solving MAX-SAT. In *Proceedings of the ICAART 2016—Proceedings of the 8th International Conference on Agents and Artificial Intelligence*, Rome, Italy, 24–26 February 2016; Volume 2, pp. 472–479.
7. Nasri, S.; Bouziri, H.; Aggoune-Mtalaa, W. Dynamic on Demand Responsive Transport with Time-Dependent Customer Load. In *Proceedings of the Innovations in Smart Cities Applications Volume 4: Lecture Notes in Networks and Systems*; Springer International Publishing: Cham, Switzerland, 2021; pp. 395–409.
8. Nasri, S.; Bouziri, H.; Aggoune-Mtalaa, W. An Evolutionary Descent Algorithm for Customer-Oriented Mobility-On-Demand Problems. *Sustainability* **2022**, *14*, 3020. [CrossRef]
9. Rezgui, D.; Siala, J.C.; Aggoune-Mtalaa, W.; Bouziri, H. Towards smart urban freight distribution using fleets of modular electric vehicles. In *Innovations in Smart Cities and Applications: Proceedings of the 2nd Mediterranean Symposium on Smart City Applications 2*; Lecture Notes in Networks and Systems; Springer: Berlin/Heidelberg, Germany, 2018; Volume 37.
10. Rezgui, D.; Bouziri, H.; Aggoune-Mtalaa, W.; Siala, J.C. A Hybrid Evolutionary Algorithm for Smart Freight Delivery with Electric Modular Vehicles. In *Proceedings of the 2018 IEEE/ACS 15th International Conference on Computer Systems and Applications (AICCSA)*, Aqaba, Jordan, 28 October–1 November 2018; pp. 1–8.
11. Rezgui, D.; Bouziri, H.; Aggoune-Mtalaa, W.; Siala, J.C. An Evolutionary Variable Neighborhood Descent for Addressing an Electric VRP Variant. In *Variable Neighborhood Search: 6th International Conference, ICVNS 2018, Sithonia, Greece, 4–7 October 2018, Revised Selected Papers 6*; Lecture Notes in Computer Science; Springer: Berlin/Heidelberg, Germany, 2019; Volume 11328, pp. 216–231.
12. Faye, S.; Melakessou, F.; Mtalaa, W.; Gautier, P.; AlNaffakh, N.; Khadraoui, D. SWAM: A Novel Smart Waste Management Approach for Businesses using IoT. In *Proceedings of the TESCA’19: Proceedings of the 1st ACM International Workshop on Technology Enablers and Innovative Applications for Smart Cities and Communities*, New York, NY, USA, 13–14 November 2019; p. 38. [CrossRef]
13. Mohapatra, H.; Mohanta, B.K.; Nikoo, M.R.; Daneshmand, M.; Gandomi, A.H. MCDM Based Routing for IoT Enabled Smart Water Distribution Network. *IEEE Internet Things J.* **2023**, *10*, 4271–4280. [CrossRef]
14. Fernandez-Prieto, J.A.; Canada-Bago, J.; Birkel, U. A Fuzzy Rule-Based System to Infer Subjective Noise Annoyance Using an Experimental Wireless Acoustic Sensor Network. *Smart Cities* **2022**, *5*, 1574–1589. [CrossRef]

15. Mohapatra, H. Socio-technical Challenges in the Implementation of Smart City. In Proceedings of the 2021 International Conference on Innovation and Intelligence for Informatics, Computing, and Technologies (3ICT), Zallaq, Bahrain, 29–30 September 2021; pp. 57–62. [CrossRef]
16. Jonek-Kowalska, I. Assessing the Effectiveness of Air Quality Improvements in Polish Cities Aspiring to be Sustainably Smart. *Smart Cities* **2023**, *6*, 510–530. [CrossRef]
17. Karagulian, F.; Barbieri, M.; Kotsev, A.; Spinelle, L.; Gerboles, M.; Lagler, F.; Redon, N.; Crunaire, S.; Borowiak, A. Review of the Performance of Low-Cost Sensors for Air Quality Monitoring. *Atmosphere* **2019**, *10*, 506. [CrossRef]
18. Ameer, S.; Shah, M.A.; Khan, A.; Song, H.; Maple, C.; Islam, S.U.; Asghar, M.N. Comparative Analysis of Machine Learning Techniques for Predicting Air Quality in Smart Cities. *IEEE Access* **2019**, *7*, 128325–128338. [CrossRef]
19. Kumar, R.; Peuch, V.H.; Crawford, J.H.; Brasseur, G. Five Steps to Improve Air-Quality Forecasts. 2018. Available online: <https://www.nature.com/articles/d41586-018-06150-5> (accessed on 12 January 2023).
20. Lin, C.; Huang, R.J.; Ceburnis, D.; Buckley, P.; Preissler, J.; Wenger, J.; Rinaldi, M.; Facchini, M.C.; O'Dowd, C.; Ovadnevaite, J. Extreme air pollution from residential solid fuel burning. *Nat. Sustain.* **2018**, *1*, 512. [CrossRef]
21. Belis, C.; Karagulian, F.; Larsen, B.R.; Hopke, P. Critical review and meta-analysis of ambient particulate matter source apportionment using receptor models in Europe. *Atmos. Environ.* **2013**, *69*, 94–108. [CrossRef]
22. Yarkin, S.; Bayram, A. Elemental composition and sources of particulate matter in the ambient air of a Metropolitan City. *Atmos. Res.* **2007**, *85*, 126–139. [CrossRef]
23. Salcedo, R.; Ferraz, M.A.; Alves, C.; Martins, F. Time-series analysis of air pollution data. *Atmos. Environ.* **1999**, *33*, 2361–2372. [CrossRef]
24. Broday, D.M. Studying the time scale dependence of environmental variables predictability using fractal analysis. *Environ. Sci. & Technol.* **2010**, *44*, 4629–4634.
25. Meraz, M.; Rodriguez, E.; Femat, R.; Echeverria, J.; Alvarez-Ramirez, J. Statistical persistence of air pollutants (O₃, SO₂, NO₂ and PM₁₀) in Mexico City. *Phys. A Stat. Mech. Its Appl.* **2015**, *427*, 202–217. [CrossRef]
26. Chen, Z.; Barros, C.P.; Gil-Alana, L.A. The persistence of air pollution in four mega-cities of China. *Habitat Int.* **2016**, *56*, 103–108. [CrossRef]
27. Meraz, M.; Alvarez-Ramirez, J.; Echeverria, J. Asymmetric correlations in the ozone concentration dynamics of the Mexico City Metropolitan Area. *Phys. A Stat. Mech. Its Appl.* **2017**, *471*, 377–386. [CrossRef]
28. Telesca, L.; Caggiano, R.; Lapenna, V.; Lovallo, M.; Trippetta, S.; Macchiato, M. The Fisher information measure and Shannon entropy for particulate matter measurements. *Phys. A Stat. Mech. Its Appl.* **2008**, *387*, 4387–4392. [CrossRef]
29. Telesca, L.; Caggiano, R.; Lapenna, V.; Lovallo, M.; Trippetta, S.; Macchiato, M. Analysis of dynamics in Cd, Fe, and Pb in particulate matter by using the Fisher–Shannon method. *Water Air Soil Pollut.* **2009**, *201*, 33–41. [CrossRef]
30. Telesca, L.; Lovallo, M. Complexity analysis in particulate matter measurements. *Comput. Ecol. Softw.* **2011**, *1*, 146.
31. Amato, F.; Laib, M.; Guignard, F.; Kanevski, M. Analysis of air pollution time series using complexity-invariant distance and information measures. *Phys. A Stat. Mech. Its Appl.* **2020**, *547*, 124391. [CrossRef]
32. R. Lamm, E.C. Rural Roads Speed Inconsistencies Design Methods. In *Research Report for the State University of New York*; Research Foundation: Albany, NY, USA, 1987; Volume Parts I and II.
33. Agency Environment Agency. Current Speed Limit Policies-Mobility and Transport-European Commission. 2008. https://road-safety.transport.ec.europa.eu/eu-road-safety-policy/priorities/safe-road-use/safe-speed/archive/current-speed-limit-policies_en (accessed on 12 January 2023).
34. Hastie, T.; Tibshirani, R.; Friedman, J. Unsupervised Learning. In *The Elements of Statistical Learning: Data Mining, Inference, and Prediction*; Springer New York: New York, NY, USA, 2009; pp. 485–585.
35. Montero, P.; Vilar, J.A. TSclust: An R Package for Time Series Clustering. *J. Stat. Softw.* **2014**, *62*, 1–43. [CrossRef]
36. Warren Liao, T. Clustering of time series data—A survey. *Pattern Recognit.* **2005**, *38*, 1857–1874. [CrossRef]
37. Partitioning Around Medoids (Program PAM). In *Finding Groups in Data*; John Wiley & Sons, Ltd.: Hoboken, NJ, USA, 1990; Chapter 2, pp. 68–125. [CrossRef]
38. Jain, A.K. Data clustering: 50 years beyond K-means. *Pattern Recognit. Lett.* **2010**, *31*, 651–666. [CrossRef]
39. Golay, X.; Kollias, S.; Stoll, G.; Meier, D.; Valavanis, A.; Boesiger, P. A new correlation-based fuzzy logic clustering algorithm for FMRI. *Magn. Reson. Med.* **1998**, *40*, 249–260. [CrossRef] [PubMed]

Disclaimer/Publisher's Note: The statements, opinions and data contained in all publications are solely those of the individual author(s) and contributor(s) and not of MDPI and/or the editor(s). MDPI and/or the editor(s) disclaim responsibility for any injury to people or property resulting from any ideas, methods, instructions or products referred to in the content.